

## SUPPORTING INFORMATION

# Towards sustainable polymeric nano-carriers and surfactants: facile low temperature enzymatic synthesis of bio-based amphiphilic copolymers in $scCO_2$

S. Curia, S.M. Howdle\*

Corresponding author: Tel.: +44 (0)115 951 3486; fax: +44 (0)115 846 8459; email: Steve.Howdle@nottingham.ac.uk

## 1 $^1H$ -NMR of copolymers

NMR studies (in  $CDCl_3$ ) showed successful controlled polymerisations for all the polymers since integrals of the peaks at 3.38 ppm (terminal methoxy group in each of the MPEG blocks) and at 4.05, 2.28, 1.63 and 1.38-1.32 ppm (PHAz backbone protons) give a molar mass that agrees with the theoretical value (Figure 1Figure 2Figure 3).

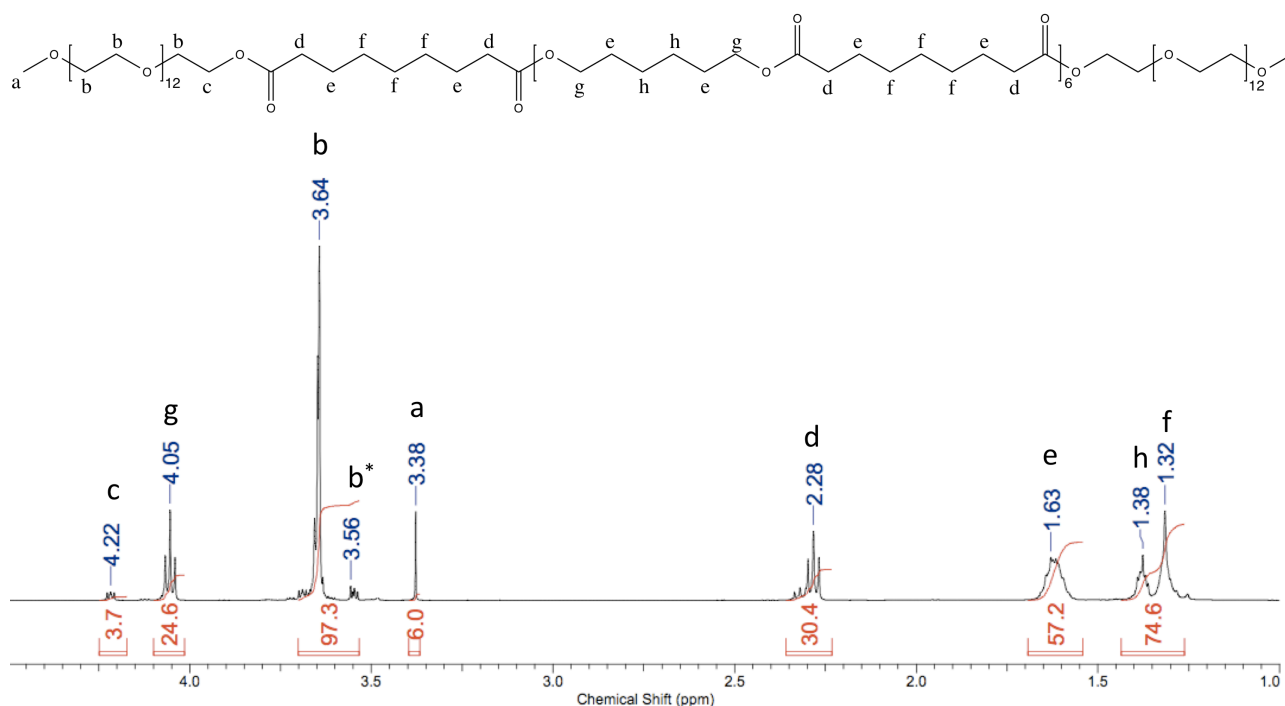


Figure 1 -  $^1H$ -NMR of polymer (b) MPEG<sub>12</sub>-PHAz<sub>6</sub>-MPEG<sub>12</sub>. Integrals of the peak at 3.38 ppm (terminal methoxy group) and 4.05, 2.28, 1.63 and 1.38-1.32 ppm (PHAz backbone) can be used to estimate the average

molar mass of the polymer. The peak b (3.64 ppm) is assigned to the  $-\text{CH}_2-$  in the MPEG backbone, while the peak b\* (3.55 ppm) is assigned to the  $-\text{CH}_2-$  protons directly attached to the terminal methoxy group ( $-\text{O}-\text{CH}_3$ ).

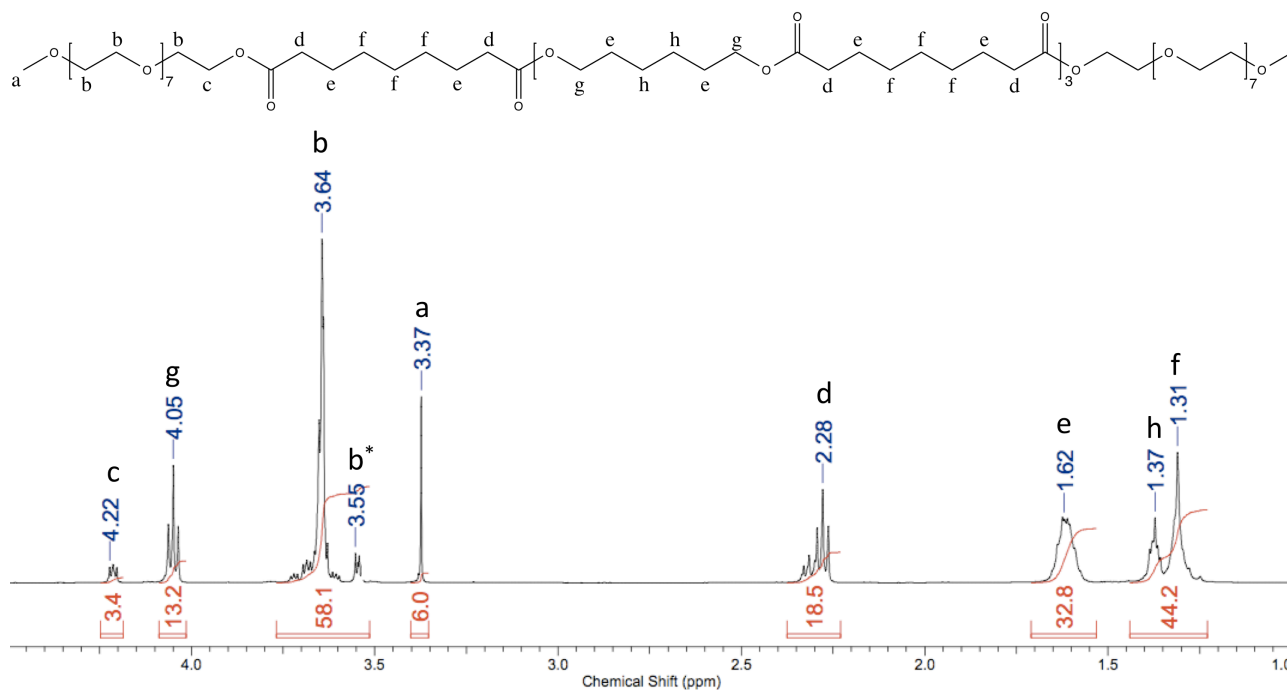


Figure 2 - <sup>1</sup>H-NMR of polymer (c) MPEG<sub>7</sub>-PHAz<sub>3</sub>-MPEG<sub>7</sub>.

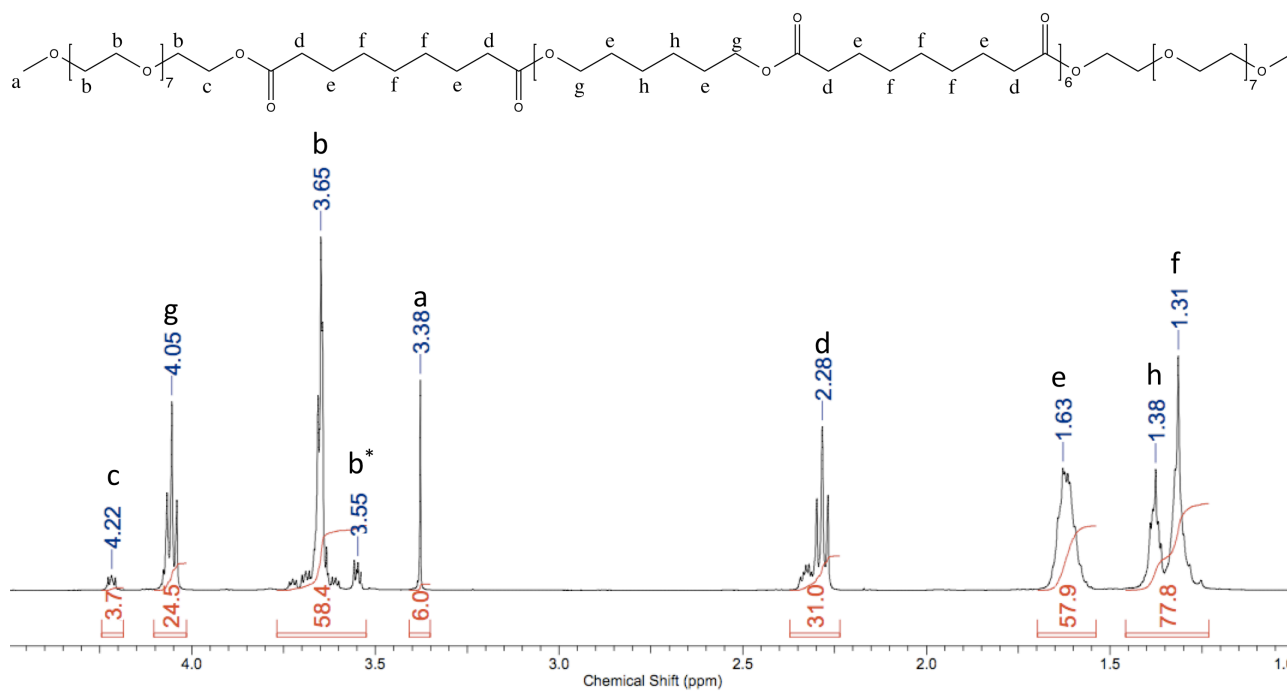
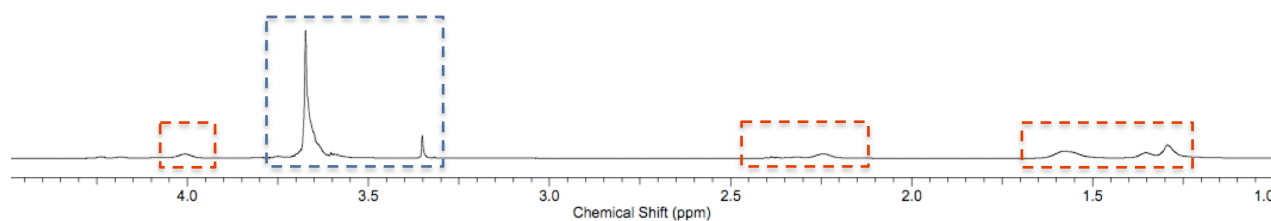


Figure 3 - <sup>1</sup>H-NMR of polymer (d) MPEG<sub>7</sub>-PHAz<sub>6</sub>-MPEG<sub>7</sub>.

In the  $^1\text{H-NMR}$  spectrum of (b)  $\text{MPEG}_{12}\text{-PHAz}_6\text{-MPEG}_{12}$  in  $\text{D}_2\text{O}$  the PHAz peaks are strongly suppressed due to the core-shell structure of the micelles (Figure 4).

## MPEG-PHAz-MPEG



**Figure 4 -  $^1\text{H-NMR}$  of polymer (b)  $\text{MPEG}_{12}\text{-PHAz}_6\text{-MPEG}_{12}$  in  $\text{D}_2\text{O}$ . The PHAz resonances are strongly suppressed, whilst the MPEG peaks are clearly observed.**

## 2 DSC studies

DSC analyses showed two endothermic peaks for the polymers (a) and (b), whilst only one peak (assigned to the PHAz crystallites) was observed for (c) and (d) (Figure 5). It is postulated that the MPEG550 blocks in (a) and (b) were long enough to undergo significant crystallisation.

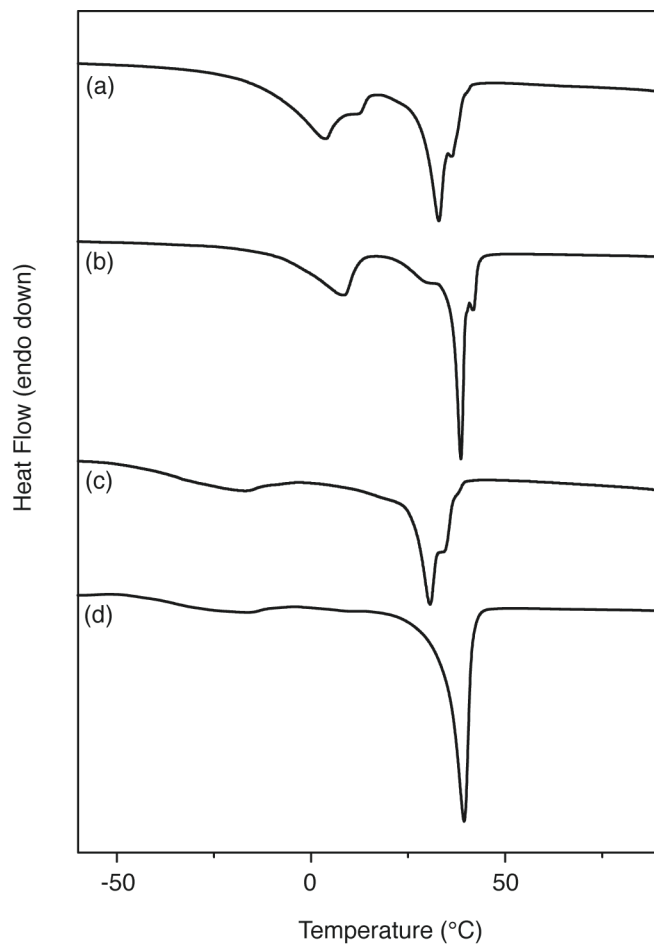


**Figure 5 – DSC traces of the copolymers: (a) MPEG<sub>12</sub>-PHAz<sub>3</sub>-MPEG<sub>12</sub>, (b) MPEG<sub>12</sub>-PHAz<sub>6</sub>-MPEG<sub>12</sub>, (c) MPEG<sub>7</sub>-PHAz<sub>3</sub>-MPEG<sub>7</sub>, (d) MPEG<sub>7</sub>-PHAz<sub>3</sub>-MPEG<sub>7</sub>. The 2<sup>nd</sup> heating scans are shown.**

### **3 DLS studies**

Intensity, volume and distribution obtained from DLS are slightly overestimated since the samples were not monodisperse. For this reason, the number distributions (shown in the paper) matched better with the TEM images. This was more marked for samples (b) and (c) (shown) since their distribution was not monomodal (Figure 6, 7, 8 and 9).

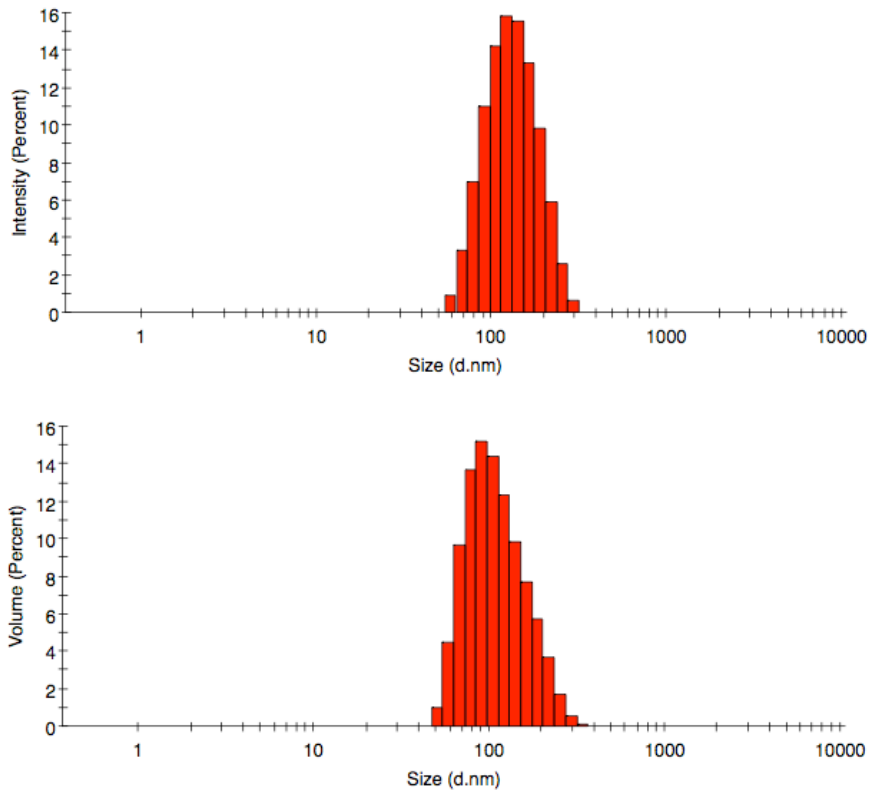


**Figure 6 – Intensity (top) and volume (bottom) distribution for (a) MPEG<sub>12</sub>-PHAz<sub>3</sub>-MPEG<sub>12</sub> micelles (0.1% wt in water).**

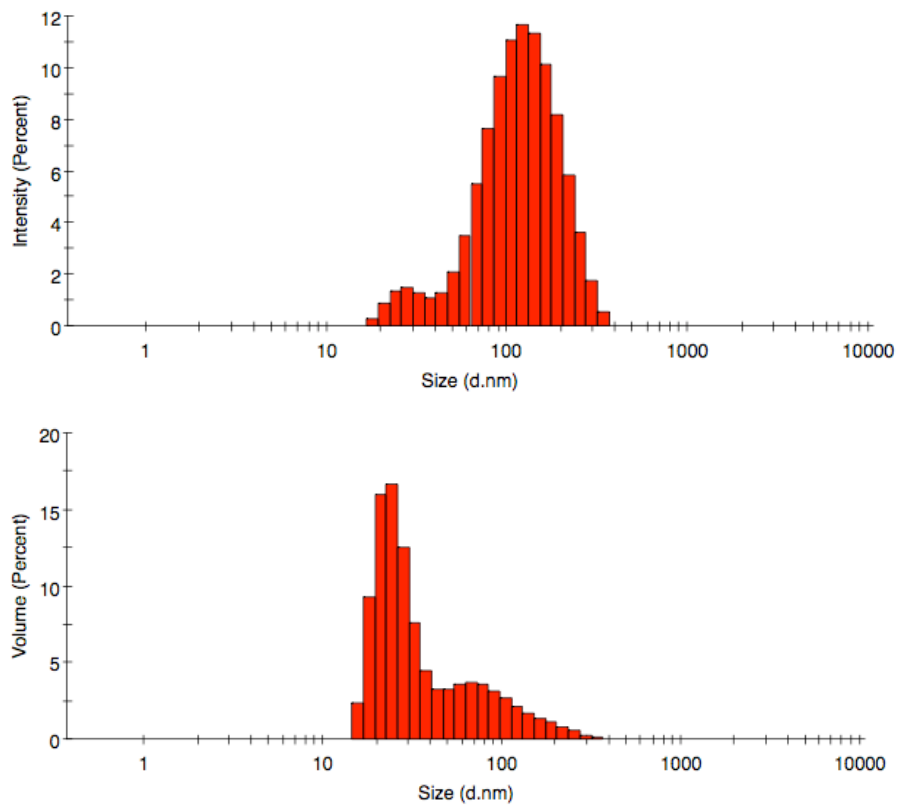


**Figure 7 - Intensity (top) and volume (bottom) distribution for (b) MPEG<sub>12</sub>-PHAz<sub>6</sub>-MPEG<sub>12</sub> micelles (0.1% wt in water).**

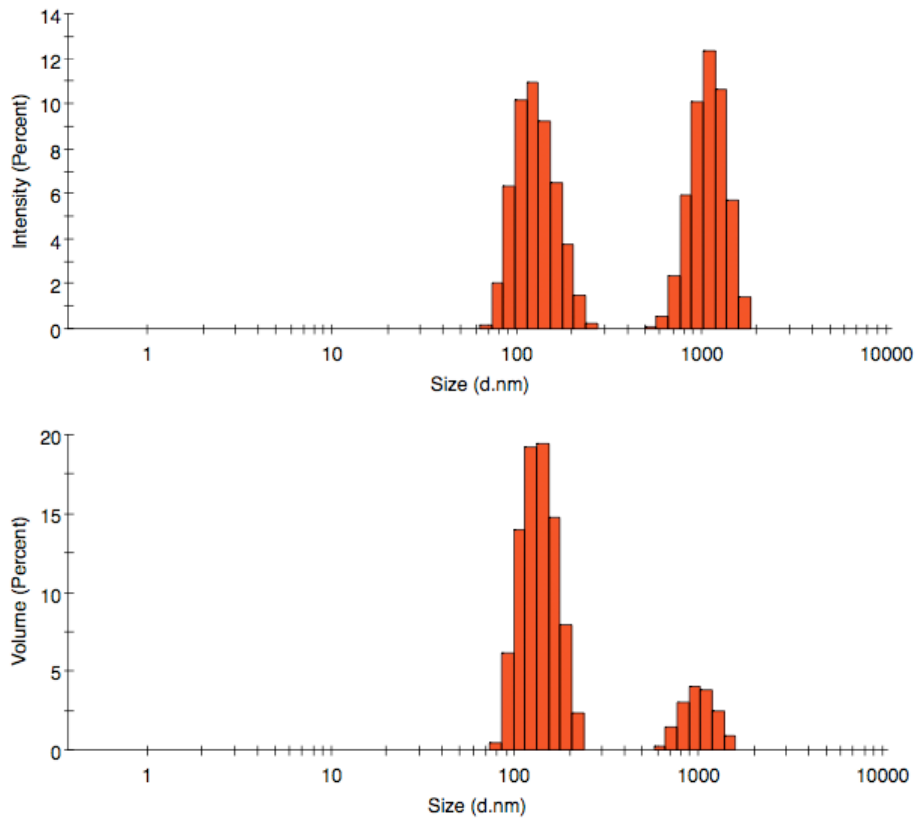


**Figure 8 - Intensity (top) and volume (bottom) distribution for (c) MPEG<sub>7</sub>-PHAz<sub>3</sub>-MPEG<sub>7</sub> micelles (0.1% wt in water).**

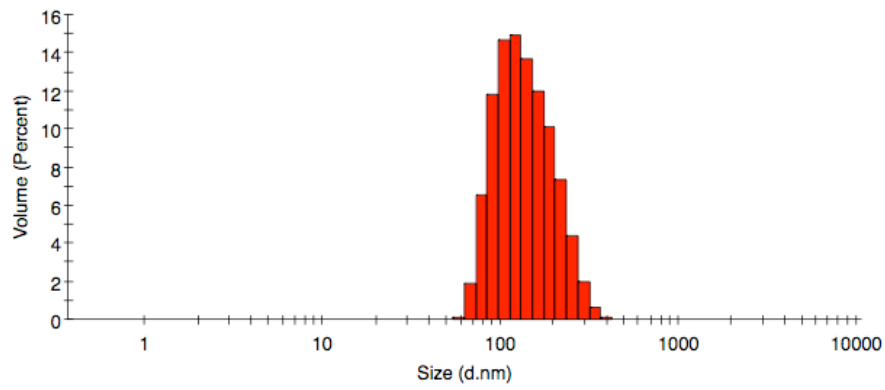
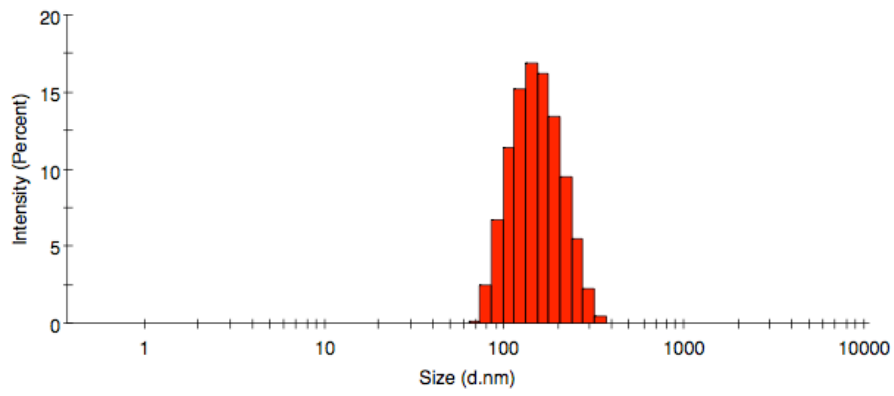


**Figure 9 - Intensity (top) and volume (bottom) distribution for (d) MPEG<sub>7</sub>-PHAz<sub>6</sub>-MPEG<sub>7</sub> micelles (0.1% wt in water).**

#### 4 Additional TEM images

As shown in the manuscript, our preliminary studies confirmed the formation of self-assembled nanometric aggregates in water. Varied aggregates were observed. Additional TEM images are shown here (Figure 10).

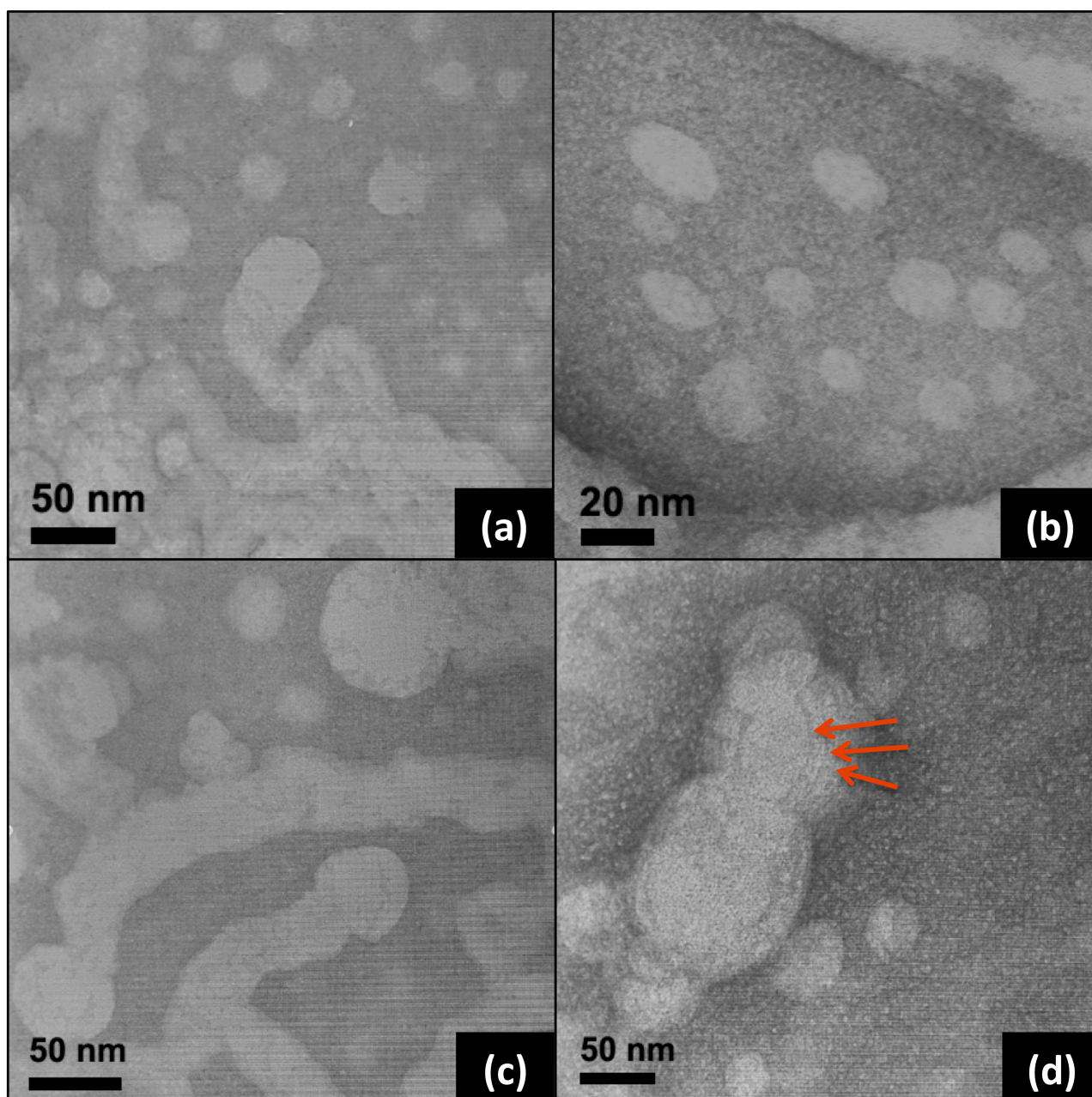
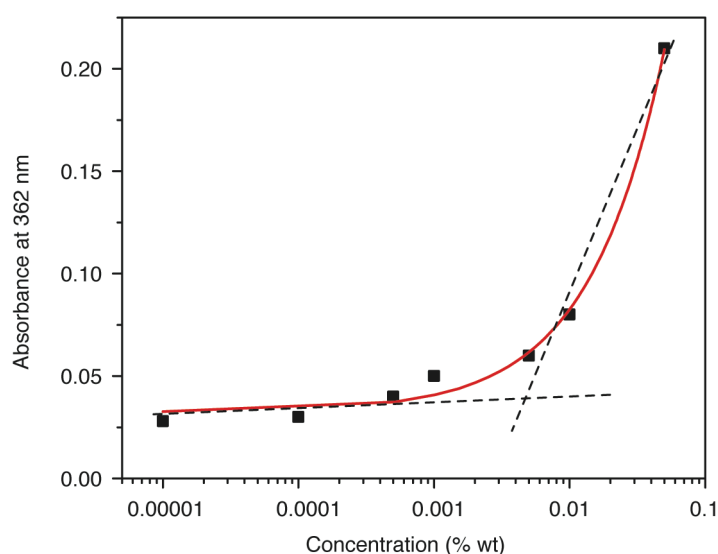


Figure 10 – Additional TEM images (taken with negative uranyl acetate staining) of: (a) MPEG<sub>12</sub>-PHAz<sub>3</sub>-MPEG<sub>12</sub>, (b) MPEG<sub>12</sub>-PHAz<sub>6</sub>-MPEG<sub>12</sub>, (c) MPEG<sub>7</sub>-PHAz<sub>3</sub>-MPEG<sub>7</sub>, (d) MPEG<sub>7</sub>-PHAz<sub>3</sub>-MPEG<sub>7</sub>. Note the possible membrane structure (red arrows) detected in polymer (d), which might indicate the presence of vesicles.

Polymer (a) and (c) show the presence of few spherical micelles, aggregated micelles and some considerably large wormlike micelles, which can be formed upon fusion of smaller spherical micelles. Polymer (b) displays only non-aggregated spherical micelles with diameters approximately ranging from 10 to 25 nm. Finally, the micrograph of polymer (d) shows some large aggregates where a tenuous concentric pattern is detected (red arrows), which might indicate the presence vesicles.

## 5 CMC studies

The CMC of was determined from the absorption of 1,6-diphenyl-1,3,5-hexatriene at a fixed concentration (0.004 mM) with increasing polymer concentration. The absorbance at 362 nm vs concentration (% wt) for polymers (a), (c) and (d) is shown (Figure 11, 12 and 13). The data were fitted with a logistic growth function (red line), whilst the CMC was determined as the crossing point of the extrapolated lines at low and high concentration.



**Figure 11 – Determination of CMC by extrapolation method for polymer (a) MPEG<sub>12</sub>-PHAz<sub>3</sub>-MPEG<sub>12</sub>.**

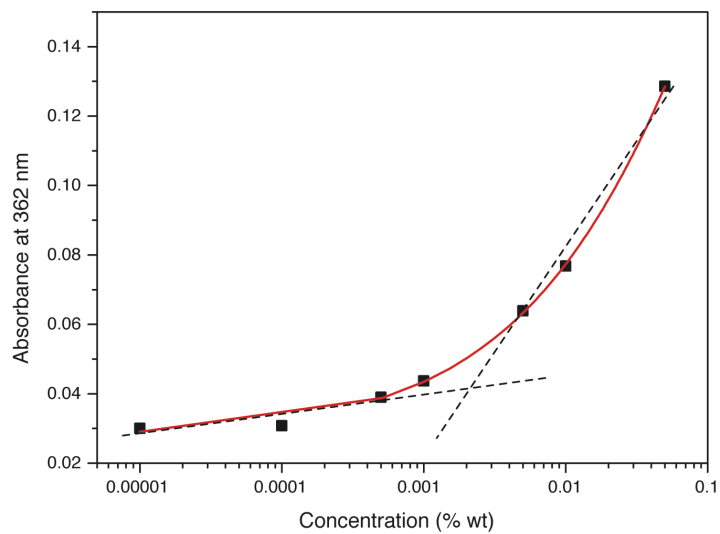


**Figure 12 – Determination of CMC by extrapolation method for polymer (c) MPEG<sub>7</sub>-PHAz<sub>3</sub>-MPEG<sub>7</sub>.**

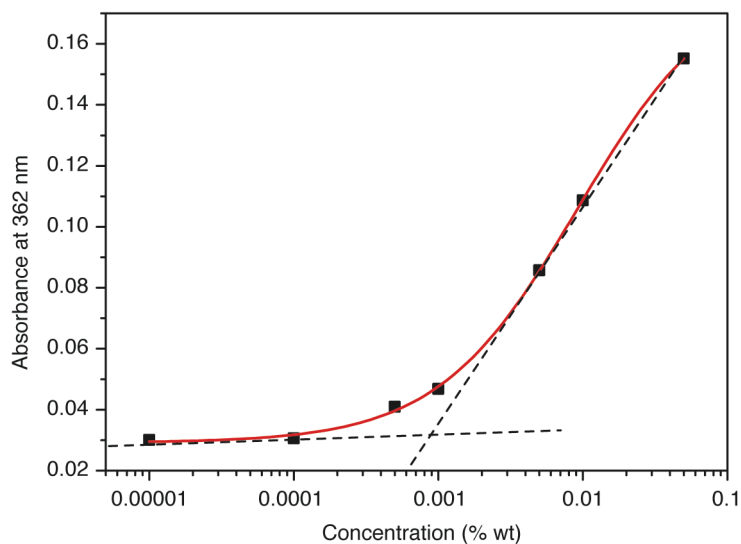


**Figure 13 - Determination of CMC by extrapolation method for polymer (d) MPEG<sub>7</sub>-PHAz<sub>6</sub>-MPEG<sub>7</sub>.**